Molecular Crystals and Liquid Crystals Science and Technology. Section A. Molecular Crystals and Liquid Crystals

Publication details, including instructions for authors and subscription information:
http://www.tandfonline.com/loi/gmcl19

The Experimental Spin Density of Two Nitrophenyl Nitroxides: A Nitronyl Nitroxide and an Imino Nitroxide

M. Bonnet [a], D. Luneau [b], E. Ressouche [a], P. Rey [b], J. Schweizer [a], M. Wan [c], H. Wang [c] & A. Zheludev [a d]

[a] CEA/DRFMC/SPSMS/MDN,CENG, 17 rue des Martyrs, 38054, Grenoble, Cedex 9, France

[b] CEA/DRFMC/SESAM, CENG, 17 rue des Martyrs, 38054, Grenoble, Cedex 9, France

[c] Institute of Chemistry, Academia Sinica, Beijing, 100080, China

[d] Brookhaven National Laboratory, Upton, NY, 11973, USA

Version of record first published: 24 Sep 2006.

To cite this article: M. Bonnet , D. Luneau , E. Ressouche , P. Rey , J. Schweizer , M. Wan , H. Wang & A. Zheludev (1995): The Experimental Spin Density of Two Nitrophenyl Nitroxides: A Nitronyl Nitroxide and an Imino Nitroxide, Molecular Crystals and Liquid Crystals Science and Technology. Section A. Molecular Crystals and Liquid Crystals, 271:1, 35-53

To link to this article: http://dx.doi.org/10.1080/10587259508034037

Mol. Cryst. Liq. Cryst., 1995, Vol. 271, pp. 35–53
Reprints available directly from the publisher
Photocopying permitted by license only

THE EXPERIMENTAL SPIN DENSITY OF TWO NITROPHENYL NITROXIDES : A NITRONYL NITROXIDE AND AN IMINO NITROXIDE.

M. BONNET[a], D.LUNEAU[b], E. RESSOUCHE[a], P. REY[b], J.SCHWEIZER[a], M. WAN[c], H.WANG[c], A. ZHELUDEV[a]*

(a)CEA/DRFMC/SPSMS/MDN,CENG,17 rue des Martyrs,38054 Grenoble Cedex 9, France

(b)CEA/DRFMC/SESAM, CENG, 17 rue des Martyrs, 38054 Grenoble Cedex 9, France

(c)Institute of Chemistry, Academia Sinica, Beijing 100080, China

Abstract We have determined, by polarized neutron diffraction, the spin density of two nitrophenyl nitroxides: the para-nitrophenyl nitronyl nitroxide (p-NPNN), which is a ferromagnet at low temperature, and the meta-nitrophenyl imino nitroxide (m-NPIN), which exhibits antiferromagnetic coupling. Several methods were used to reconstruct the spin density distribution, including the maximum entropy method. Our data provide the basis for a better knowledge of the electronic configuration. The nodes of the SOMO are directly observed and the spin polarization effects which give rise to a negative spin density on several atomic sites is discussed.

INTRODUCTION

Conjugated nitroxide free radicals are among the most widely used spin carriers in the design of magnetic molecular compounds. As their unpaired electron is delocalized over the different atoms of the molecule, they are convenient building blocks and ideal magnetic bridges between magnetic metals to achieve new compounds with particular magnetic properties. To grasp their role as chemical and magnetic ligands, it is essential to understand their electronic properties, and particularly to know how is the unpaired electron wave function distributed.

Among the nitroxide free radicals are the nitronyl nitroxide radicals which include two N-O groups located symmetrically on both sides of a 5-membered ring (Fig. 1(a)), and the imino nitroxide radicals with one N-O group on one side and one N atom only on

* Present adress : Brookhaven National Laboratory, Upton, NY 11973, USA.

the other side of the same ring (Fig. 1(b)). In the case of nitronyl nitroxides, the unpaired electron is supposed to be, in a first approximation, equally shared by the four atoms O, N, N and O, and the single occupied molecular orbital (SOMO) is supposed to exhibit a node on the C atom in between the two NO's (Fig. 1(a)). In the case of imino nitroxides, the unpaired electron is mainly carried by the three atoms N, N and O, but, as the symmetry is broken, no node is expected on the central C atom for the SOMO (Fig. 1(b)).

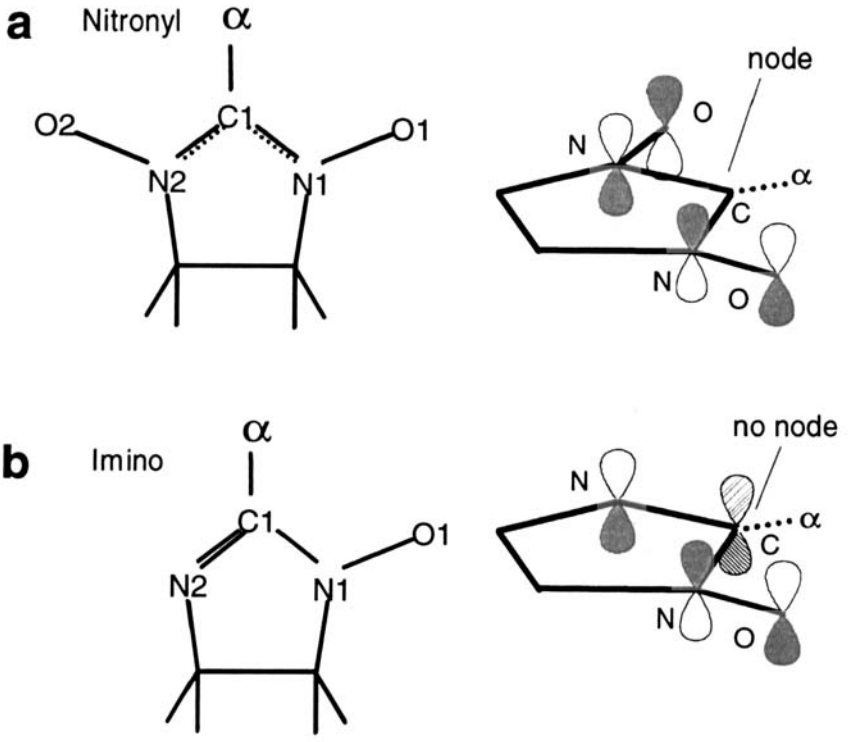

FIGURE 1 Nitroxide radicals and their SOMO wave function: (a) nitronyl nitroxide, (b) imino nitroxide.

Moreover, changing the substituant fragment α of the nitronyl or the imino nitroxides allows to tune the single radical ground state to establish intermolecular exchange pathways, providing new coordination sites. Several interesting species with a nitrophenyl substituant for the α fragment have been reported[1-6]. They may provide both antiferromagnetic or ferromagnetic intermolecular interactions.

We compare herein the spin density distribution obtained by single crystal polarized neutron investigation of two nitrophenyl nitroxides free radicals : the para-

nitrophenyl nitronyl nitroxide (p-NPNN) which is a ferromagnet below $T_C = 0.67$ K[7] and the meta-nitrophenyl imino nitroxide (mNPIN) which exhibits antiferromagnetic coupling[8].

THE EXPERIMENTAL TECHNIQUE

Polarized neutron diffraction is a technique very well adapted for measuring the spin density distribution in magnetic molecular crystalline compounds[9]. The measurements are generally performed in the paramagnetic state (above T_C in the case of a p-NPNN). A periodic spin density $\vec{S}(r)$ is induced in a single-crystal sample by applying a strong external magnetic field at a sufficiently low temperature. The induced density is aligned with the vertically applied field : $\vec{S}(r) = \hat{z}\, S(r)$ ($\hat{z}$ is the field direction). Since both the crystal structure and the induced magnetization have the same spatial periodicity, the scattering occurs at Bragg positions (hkl).

The neutrons are scattered in the crystal by two types of interactions, and the total scattered intensity is the result of the interference effect. The strongest contribution is given by the interaction of the neutrons with the nuclei, which is independent of the neutron spin. The magnetic contribution is given by the product of the neutron spin $\vec{\sigma}$ and the projection of the magnetic structure factor $\vec{F}_M(\vec{k})$ (the Fourier component of the induced spin density $\vec{S}(r)$ onto a plane perpendicular to the scattering vector $\vec{k}$:

$$\vec{\sigma}\, \vec{F}_{M\perp}(\vec{k}) = \vec{\sigma}\, (\hat{k} \wedge \hat{z} \wedge \hat{k})\, F_M \quad ; \quad \hat{k} = \vec{k} / |\vec{k}| \tag{1}$$

If a non-polarized neutron beam is used, the total scattering intensity is simply the sum of the nuclear and magnetic ones : $I = |F_N|^2 + |\vec{F}_{M\perp}(\vec{k})|^2$. The interference between the two scattering modes vanishes when an averaging over the 2 spin states of the incident neutron beam is performed. On the contrary, if the incident beam is polarized, a cross-term appears, which depends on the beam polarization vector $\vec{p}$:

$$I = |F_N|^2 + |\vec{F}_{M\perp}|^2 + 2\,\mathrm{Re}(F_N^*(\vec{p}\, \vec{F}_{M\perp})) \tag{2}$$

This interference is important in two respects: (i) in the cross-term the strong nuclear scattering amplifies the magnetic one, which is usually much weaker, enhancing the sensitivity of the method ; and (ii) by performing measurements for both polarizations of the incident neutrons one can separate the nuclear and magnetic signals and deduce the spin density distribution in the crystal. In practice one measures the so-called "flipping ratio" R of Bragg reflections, that is, the ratio of scattered intensities for "up" (parallel to the applied field) and "down" (antiparallel) polarizations of the incident beam :

$$R = \frac{I^+}{I^-} = \frac{|F_N|^2 + q^2|F_M|^2 + 2q^2\,\mathrm{Re}(F_N^* F_M)}{|F_N|^2 + q^2|F_M|^2 - 2q^2\,\mathrm{Re}(F_N^* F_M)} \qquad (3)$$
$$q^2 = 1 - (\hat{z}\hat{k})^2$$

The determination of the spin density should include two steps. In the first step, the exact crystal structure of the compound is determined. This may be done by a conventional, unpolarized, neutron diffraction experiment. The results are used to calculate the F_N's. In the second step one measures the flipping ratios with a polarized neutron beam. The spin density is then deduced from the R's and F_N's using equation (3) and its simple Fourier transform relation to the F_M's. In a non-centrosymmetric structure all the F's are complex quantities. This means that the F_M's cannot be straightforwardly obtained from solving (3) and the spin density is to be deduced directly from the R's.

EXPERIMENT

For both compounds the room temperature crystal structures were already determined by X-ray diffraction. We have refined these structures at low temperature with unpolarized neutrons, and then measured the flipping ratios with polarized neutrons.

p-NPNN

Among the 4 phases which exist for p-NPNN, only the ß phase is ferromagnetic. It crystallizes in dark purple, regularly shaped crystals, in the orthorhombic and non centric Fdd2 space group[10-11]. The low temperature neutron investigation for crystal structure refinement was performed at T = 6 K on the 4 circle diffractometer DN4 of the Siloe reactor (CEN-Grenoble). At this temperature the cell constants are a = 19.01(3) Å, b = 10.71(2) Å, c = 12.16(3) Å. The intensities of 517 independent Bragg reflections were recorded.

The polarized neutron study was then performed on the DN2 spectrometer, with an applied field of 4.65 T at temperatures of 1.6 K, 2.0 K and 4.8 K. In a first serie of experiments the crystal was mounted with the $\vec{c}$ axis vertical and parallel to the field with (hk0), (hk1), (hk2) and (hk3) reciprocal planes accessible to the measurements. In a second serie, axis $\vec{a}$ was parallel to the field and flipping ratios (0kl), (1kl), (2kl) and (3kl) were collected. Altogether 246 independent flipping ratios were measured.

m-NPIN

It crystallizes in translucent red regularly shaped crystals. The structure corresponds to the centrosymmetric monoclinic space group P $2_1/c$ [8]. The low temperature unpolarized neutron experiment was performed at T =30 K. At this temperature the cell constants were determined as : a = 13.15(3) Å, b = 7.29(2) Å, c = 26.98(4) Å and ß = 91.45(11) °. 2180 independent Bragg intensities were measured up to $\sin\theta/\lambda = 0.42$ Å^{-1}.

For the polarized neutron experiment two series of measurements were carried out at T=1.6 K. In the first series a 5.7 x 5.3 x 1.1 mm^3 crystal was mounted with the $\vec{b}$ axis collinear to the 4.65 T field of the split-coil cryomagnet. In this geometry the (h0l), (h1l) and (h2l) reciprocal planes were accessible for measurements. In the second series, the same crystal was rotated to align the $\vec{c}$ axis parallel to the field. Flipping ratios in the planes (hk0), (hk1), (hk2) and (hk4) were collected. In both series the measurements were performed for $\sin\theta/\lambda$ up to 0.38 Å^{-1}. Altogether 248 independent flipping ratios were measured.

LOW TEMPERATURE STRUCTURE REFINEMENTS

The structures were refined using the least-squares program ORXFLS[12]. Absorption corrections were made by calculating the mean crystal traversing path for each reflection.

p-NPNN

Using 481 data and 121 variables the value of $\chi^2 = 1.7$ (weighted R-factor = 7.8 %) was achieved. Anisotropic thermal parameters were refined for all but hydrogen atoms, for which isotropic thermal factors were used. Extinction turned out to be significant ; it was modeled in the approximation of a gaussian mosaic crystal. The structure is similar compared to that at room temperature. There is only one type of molecule in the crystal, and it presents the following features which are important for the discussion of the spin density:

(i)The molecule is symmetric towards a 2 fields axis passing through the central C atom and the N atom of the nitro group.

(ii)The O-N-C-N-O fragment is practically planar. It forms an angle of 49.5° with the phenyl ring (in the phenyl-substituted radical this angle was found to be # 25°) and 67.4° with the NO_2 plane.

(iii)Close intermolecular contacts between the N2 atom and the O1 atom of the neighboring molecules form a two-dimensional network parallel to the (bc) crystallographic plane, as shown in fig. 2. The N2-O1 distance is 3.225 Å. These contacts are referred to as type 1.

(iiii) The 3.137 and 3.180 Å distances between O1 and C6, C7 of the next molecule, provide links between adjacent planes. These close contacts are referred to as type 2.

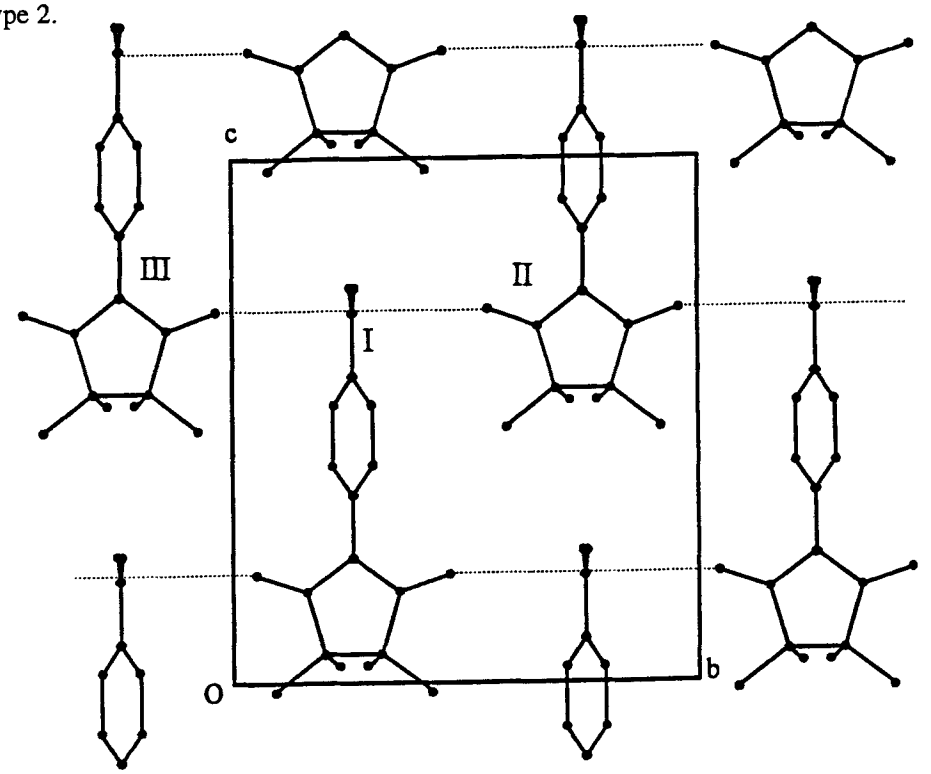

FIGURE 2 2D planes parallel to the (bc) crystallographic plane in the structure of p-NPNN

m-NPIN

Using 2180 data and 286 variables the value of $\chi^2 = 1.56$ (weighted R-factor = 9.3 % was achieved. All atoms were treated with isotropic thermal parameters. Extinction was found to be very small and was not taken into account. The structure is similar to that at room temperature. The most important features are summarized here.

(i) The asymmetric unit cell contains two m-NPIN radicals. Though crystallographically independent, the two molecules (referred to as molecules A and B), especially their imino groups, are in "nearly equivalent" positions, closely coinciding upon a 1/4 translation along the $\vec{c}$ axis. Fig. 3 shows the structure in projection onto the (ac) crystallographic plane, with the atom labeling scheme used throughout the paper.

(ii) The imino groups of the two molecules have very similar geometry. The N-C-N-O fragment is practically planar.

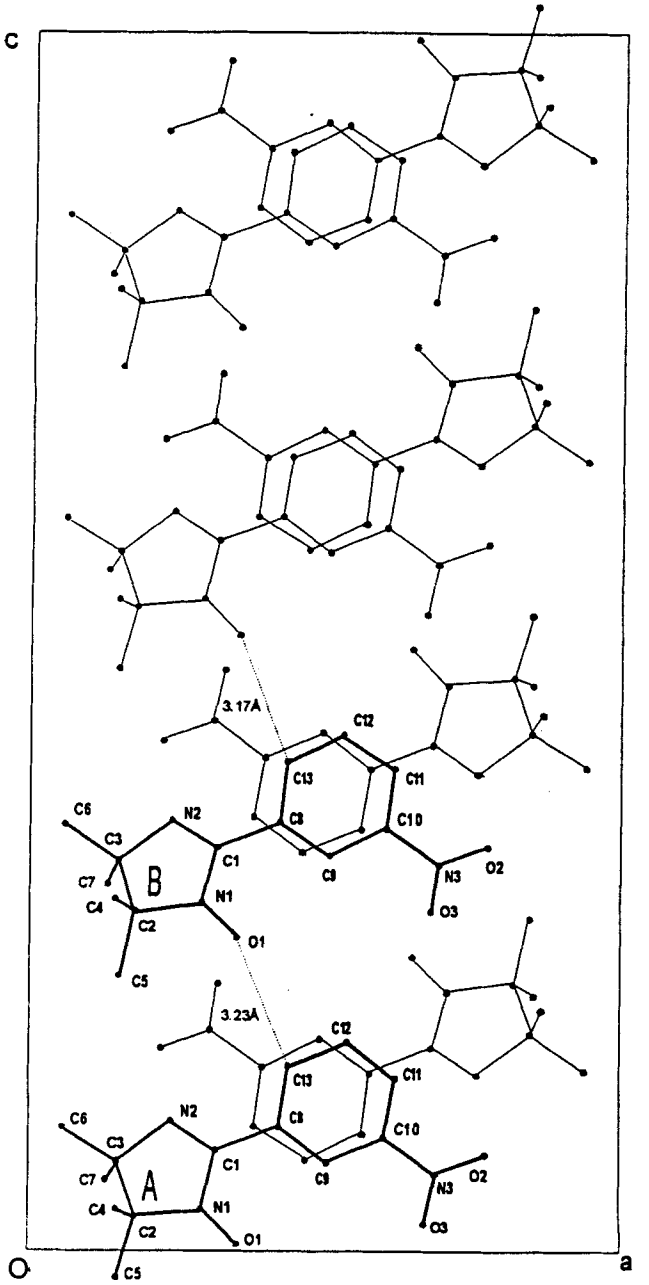

FIGURE 3 Projection onto the (ac) crystallographic plane in the structure of m-NPIN.

(iii) The main difference between A and B lies in the orientation and geometry of the nitrophenyl fragments. The interplanar angle between the mean plane of the phenyl cycle and that of the N-C-N-O fragment in A and B is 44.7° and 13.0° respectively. The nitro group plane is rotated to that of the phenyl by 5.7° and 19.2° in molecules A and B.

(iiii) The radicals are clearly organized in double chains, stretching along the $\vec{c}$ axis as shown on Fig. 4. The shortest intermolecular contacts in the structure link phenyl carbon atoms of each molecule and the O1 site of the neighbor : C13A and O1B - 3.23 Å and C13B and O1A - 3.17 Å. The contacts are marked with dashed lines on figures 3 and 4.

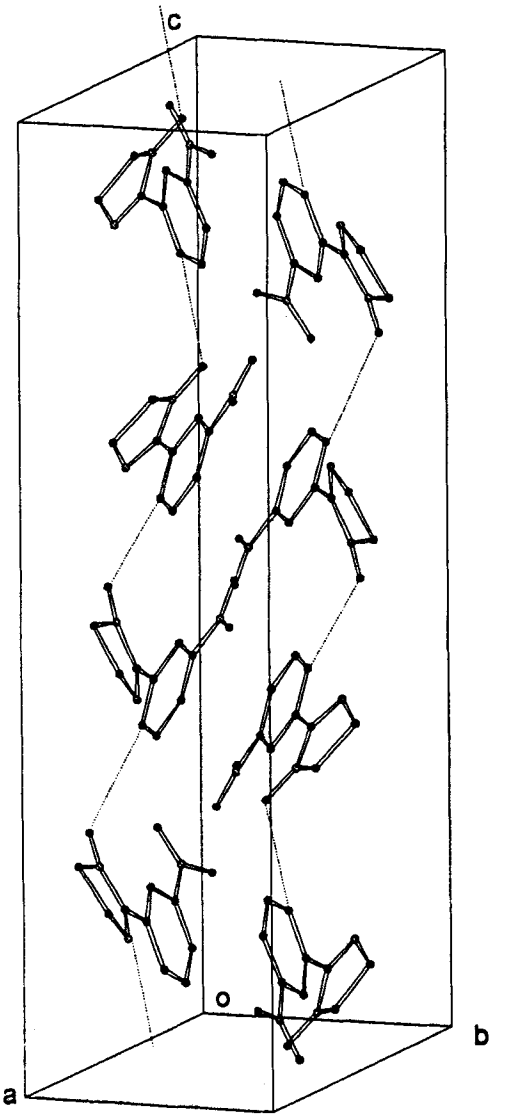

FIGURE 4 Cristal structure of m-NPIN.

DATA TREATMENT : MODELING THE SPIN DENSITY

The most general approach, to retrieve the spin density from the experimental flipping ratios, is to design a parametrized model of the spin distribution, and to refine the parameters to best fit the data. In fact this is up to now the only method available for dealing with non-centrosymmetric structures. To obtain quantitative data in terms of individual atomic spin populations and to extract information concerning the polarization of the nitrophenyl fragment, an atomic orbital model, constructed from standard Slater functions Φ_i, at each atomic site i, was used, and the spin density S(r) is expanded as :

$$S(r) = \sum_i S_i \, \Phi_i(r) \, \Phi_i^*(r) \qquad (4)$$

The individual atomic populations S_i as well as the radial exponents of the Slater wavefunctions for each orbital type are the parameters of the model which are refined to provide the best fit to the data. In this model the atomic wavefunctions are first squared, and only then a linear combination is made. In this way we allow for negative spin populations.

Theoretical calculations suggest to include $|2p_z\rangle$ orbitals on the N, O and C atoms of the O-N-C-N-O fragment. Because of its small contribution, the spin density was refined to its spherical contribution for the other carbon atom of the nitronyl or the imino group. However $|2p_z\rangle$ orbitals were chosen for both the phenyl carbons and the NO_2 group.

The models were refined using a modification of the least square program MOLLY[13]. The starting values of the Slater radial exponents were taken from Hehre et al.[14]. They were refined on the atoms of the O-N-C-N-O fragment.

p-NPNN

The data obtained at different temperatures were scaled to T=2K and H = 4.65T. The resulting populations obtained in the frame of the atomic orbital model are presented in Table I. This refinement corresponds to an agreement factor χ^2=1.2. Fig. 5 shows the level contour for the spin density projected onto the O-N-C-N-O plane. The total spin populations of the p-NPNN radical was found to be 1.00(3) μ_B, which is in agreement with the 0.97 μ_B value obtained from SQUID measurements.

m-NPIN

The limited resolution of the data does not allow the separation of the magnetic signal from the two nearly equivalent molecules A and B. Therefore, in the model which was actually refined, the spin populations of corresponding atoms of A and B were

constrained to be equal, to result in some sort of "averaged" molecule. This refinement gave an agreement factor χ^2=2.1, too large, which shows that this simple atomic orbital model is inadequate for a correct description of the spin density distribution in the radical.

TABLE I Spin populations in p-NPNN and m-NPIN.

p-NPNN		m-NPIN	
O1	0.283(7)	0.407(15)	O1
N1	0.257(7)	0.335(16)	N1
		0.236(7)	N2
C1	-0.090(9)	-0.057(10)	C1
C2	0.020(5)	0.027(9)	C2
		-0.027(11)	C3
C3	0.020(5)	0.010(7)	C4
		0.006(7)	C5
C4	-0.027(5)	0.055(11)	C6
		0.006(7)	C7
O2	-0.002(5)	-0.005(5)	O2
		0.026(7)	O3
N2	0.021(5)	-0.016(6)	N3
C5	0.000(9)	0.002(7)	C8
C6	-0.001(7)	-0.001(9)	C9
		0.002(7)	C10
C7	-0.011(7)	-0.016(7)	C11
		-0.001(7)	C12
C8	-0.008(10)	0.012(7)	C13

The flexibility of this simple model was increased by direct modeling of the spin density, instead of modeling the magnetic wave function. In the vicinity of the nuclei the spin density was expanded into a multipolar series [9]:

$$S(r) = \sum_{\ell} R^{\ell}(r) \sum_{m=-\ell}^{m=\ell} \alpha_{\ell}^{m} \, y_{\ell}^{m}(\hat{r}) \tag{5}$$

y_{ℓ}^{m} are real spherical harmonics, R^{ℓ} are standard Slater radial functions and α_{ℓ}^{m} are the population coefficients.

(i) As before, the spin distributions in the two molecules were constrained to be equal.

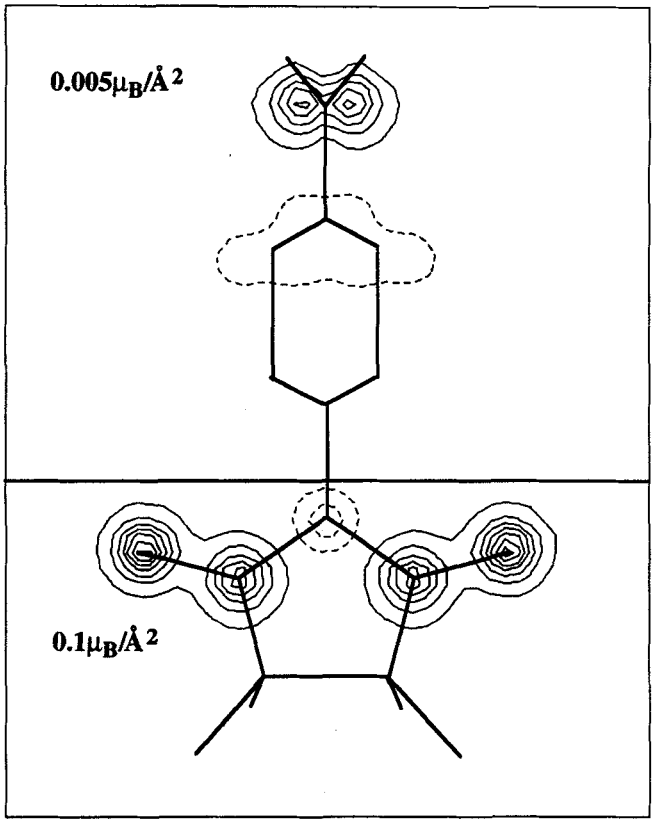

FIGURE 5 Projection of the spin density on the O-N-C-N-O plane in p-NPNN.

(ii) The expansion (5) was used only for the N1 and O1 sites, where a *strong* deformation of a *large* spin density was observed. For all the other sites the atomic orbital description of the spin density was kept.

(iii) For N1 and O1 only those spherical harmonics which are even with respect to $\hat{z}$ and $\hat{x}$ (axis $\hat{x}$ is chosen perpendicular to $\hat{z}$ and to the O1-N1 bond) and which correspond to $\ell \leq 3$ were included into the expansion.

The refined values of atomic spin populations are listed in Table I. Fig. 6 shows the obtained spin density in projection onto the N-C-N-O molecular plane. The achieved agreement with experiment $\chi^2 = 1.6$ shows that it describes the spin density in the compound much better than the one based on axially symmetrical p- orbitals.

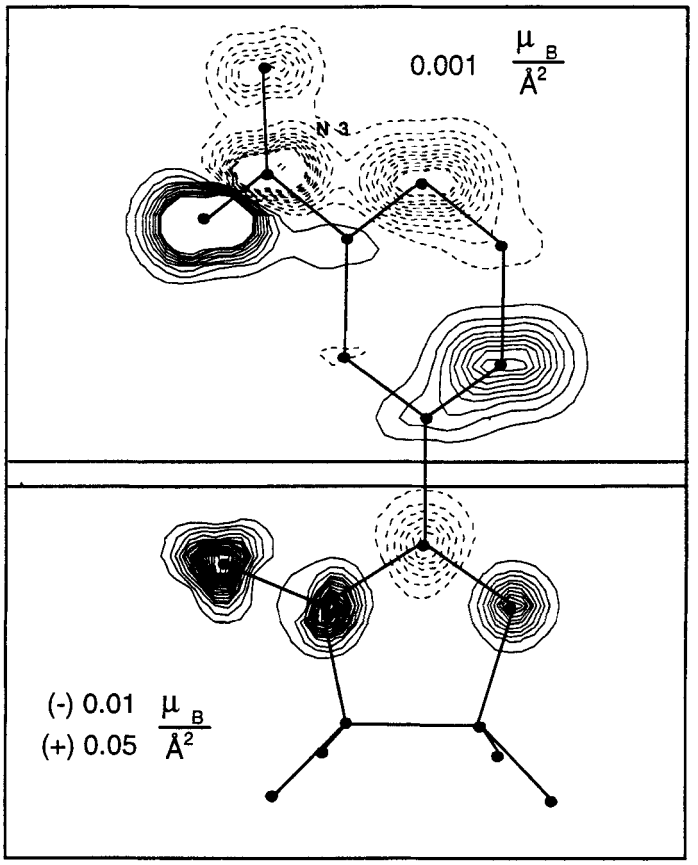

FIGURE 6 Projection of the spin density onto the N-C-N-O plane in p-NPIN.

DATA TREATMENT: MODEL INDEPENDENT SPIN DENSITY RECONSTRUCTION

Model-independent methods (Fourier inversion among them) allow to reconstruct the spin density without involving any additional knowledge of what the result should look like. Since the $F_M(h,k,l)$ are the Fourier components of the spin density $S(x,y,z)$, the task of spin density reconstruction is an inverse Fourier problem. The usual and straightforward approach to solve such a problem is to calculate the inverse Fourier sum:

$$S(x,y,z) = \frac{1}{V} \sum_{h,k,l} F_M(h,k,l)\, e^{-2\pi i(hx+ky+lz)} \tag{6}$$

The sum is taken over all Bragg reflections for which the F_M's were determined. This method has been widely used to interpret polarized neutron diffraction data, but it has its drawbacks. Since not all Fourier components are known, there are in fact many possible spin density distributions (maps) which fit the data. Inverse Fourier summation selects one of them: the one with zero values for unmeasured coefficients, and values exactly in the middle of the error bars for those measured. On the contrary, the recently developed maximum of entropy (MaxEnt) technique[15-16] selects among all the maps consistent with the data the most probable one, that is the one that maximizes the Boltzmann entropy:

$$\begin{aligned} \text{Entropy}[S(x,y,z)] &= - \int_{\text{unitcell}} s(x,y,z) \ln(s(x,y,z))\, dx\, dy\, dz \\ s(x,y,z) &= \frac{S(x,y,z)}{\int_{\text{unitcell}} S(x,y,z)\, dx\, dy\, dz} \end{aligned} \tag{7}$$

The formula applies to strictly positive distributions, but the method is easily modified to treat sign alternating densities. In practice one maximizes the functional (7) under the constraints $\chi^2 \leq 1$. This method is known to give much better results than conventional Fourier inversion and is also model independent.

p-NPNN

Even though the structure of p-NPNN is non centrosymmetric, a projection onto the (ab) plane has a center of symmetry at the origin. Thus all the structure factors of the (hk0) Bragg reflections are real and the F_M's may be obtained directly from the experimental flipping ratios by solving Eq. (3).

The F_M's obtained from (3) were all scaled to T = 2K and H = 4.65 T in accordance with the SQUID results. The MaxEnt reconstructed projected spin density is presented in Fig. 7. Several important features are to be emphasized here:

(i) The majority of spin resides on the N1 and O1 atoms and is shared equally between those sites.

(ii) The shape of the spin density is observed directly, that is, without introducing any model in the data treatment. Definite p_z orbital shapes are evidenced, but not exactly centered on the N1 and O1 atoms.

(iii) Practically no spin density is observed on the rest of the nitrophenyl group. This does not mean that those contributions are vanishingly small. MaxEnt tends to smooth out all the weak contributions, emphasizing the main spin density peaks. This is

reinforced as only 41 (hk0) type reflections of the 246 measured (hkl) reflections were used in this reconstruction.

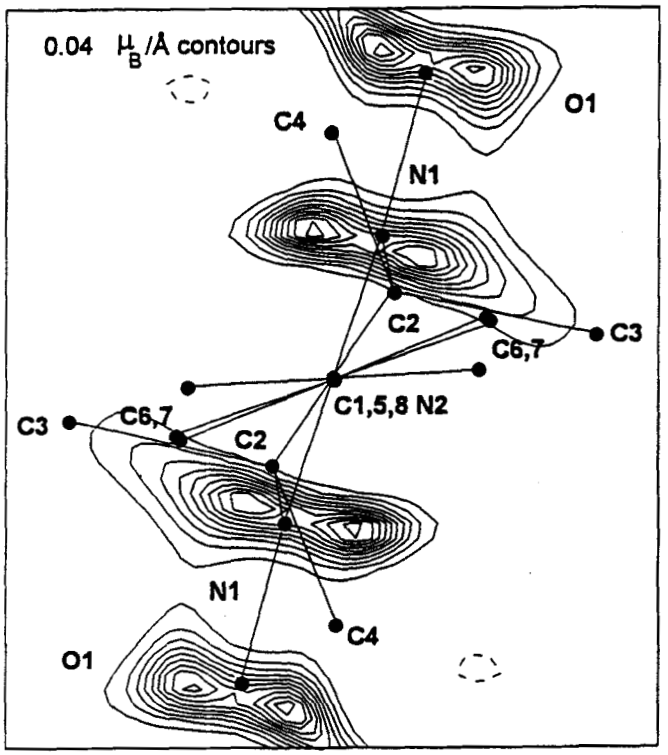

FIGURE 7 Maxent reconstruction of the spin density in p-NPNN projected onto the (ab) molecular plane.

m-NPIN

The spin distribution, obtained by MaxEnt is presented on Fig.8 in projection onto the O-N-N planes for each of the two molecules. The important features, which are observed on both molecules, are:

(i) The majority of the spin resides on the N1, N2 and O1 atoms, equally shared between those sites.

(ii) On the N1 and O1 sites of both molecules the density is not centered on the nuclei but is slightly shifted away from the center of the N1-O1 bond. The effect is more pronounced on the N1 site.

(iii) On the central C1 carbon atoms the spin density is *negative*. Moreover, it is off-centered, shifted in the N1-N2 direction.

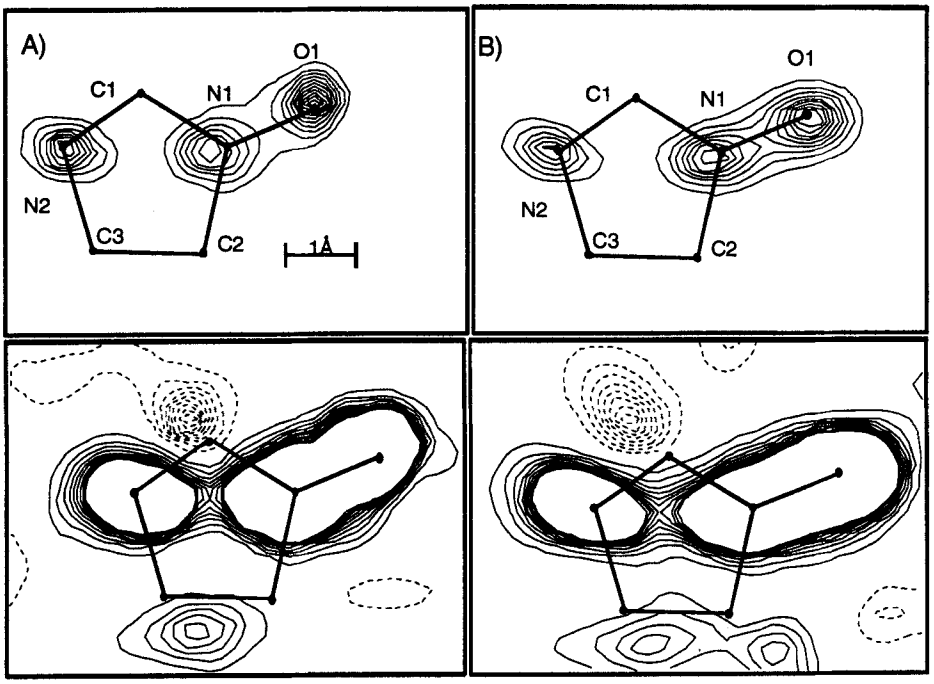

FIGURE 8 Maxent reconstruction of the spin density in p-NPIN projected onto the N-C-N-O plane for the two molecules A and B. 0.05$\mu_B/Å^2$ (above) and 0.003$\mu_B/Å^2$ (below) contour steps.

DISCUSSION

The imino and the nitronyl nitroxide fragments

For the two radicals most of the spin density lies on the nitrogen and the oxygen atoms, as expected for the single occupied molecular orbital (SOMO) in such radicals. In the nitronyl radical, the density is almost equally shared by the four O,N,N,O atoms, as already found in the simple phenyl nitronyl nitroxide (PNN) crystal[17]. For the imino radical, the lack of one of the oxygen atoms breaks the symmetry and pushes all the spin distribution towards the remaining oxygen. Such an effect was already observed when

the PNN radical was equatorially and antiferromagnetically bounded to a copper atom[18]. This resulted in the disappearance of the spin density on the bonding oxygen, and a general shift of all the distribution towards the other oxygen atom.

For the two compounds, the antibonding character of the SOMO appears clearly on the spin density maps when reconstructed by the maximum entropy method. Around the N and O atoms (figures 7 and 8), the spin density is clearly built from 2p orbitals, but these 2p orbitals are slightly bent and pushed away from the center of the N-O groups. These features do not appear on the maps obtained by the orbital modeling of the spin density (fig. 5) as this parametrized model is not flexible enough to include such an off centering. The reality of this deformation has been carefully checked in the m-NPIN crystal by a new development of the maximum entropy method, including a reference model in the definition of the entropy [19]. The off centering is real and occurs as well in the molecule A as in the molecule B [20].

A significant amount of negative spin density is found on the sp^2 carbon. In the p-NPNN radical, this atom is located on a node of the SOMO. To account for this effect one has to go beyond the restricted Hartree-Fock scheme, introducing exchange interactions and spin polarization effects. Those are conveniently described in terms of configuration interactions, as HOMO-LUMO excitations, induced by the unpaired spin on the SOMO. These frontier orbitals of the nitroxide group have a large contribution from an atomic $|2p_z>$ orbital on this carbon atom, which becomes polarized, and negative.

In m-NPIN, the central carbon is no more a node of the SOMO and there is no a priori reason for its spin population to be small or negative. Experimentally it is observed negative and off centered from the carbon nucleus. This is the result of a competition between spin polarization and spin delocalization. Both are of the same order of magnitude, the spin polarization being slightly larger, providing a negative total density. This competition of two opposite effects explains the observed off centering. The SOMO has 2 nodes. One node is clearly located between N1 and O1 and the other one probably between C1 and N2, making C1-N1 bonding and C1-N2 antibonding. Therefore, the positive contribution to the spin density on C1 becomes shifted along the N2-N1 direction. On the other hand, the polarization of the frontier orbitals, which is liable for the negative contribution, is distributed in the following way : the lowest unoccupied orbital (LUMO) is antibonding on both C1-N1 and C1-N2, which corresponds to a shift in the C1-C8 direction; the highest occupied orbital (HOMO) is bonding on C1-N2 and *antibonding on C1-N1*, which means a shift along N1-N2. As the negative contribution dominates, the total spin density becomes deformed and shifts in a direction intermediate between N1-N2 and C1-C8, as seen in figure 8.

The nitrophenyl group

A former study on the simple phenyl nitronyl nitroxide (PNN) radical[18] had shown the familiar sign alternating +-+-+ spin populations on the carbon atoms of the phenyl ring. In the investigated crystal, the PNN molecules were far enough one from the other, to avoid magnetic coupling. In the two nitrophenyl nitroxide radicals which are discussed here, the neighboring molecules are close enough to present magnetic interactions: ferromagnetic for p-NPNN and antiferromagnetic for m-NPIN. These interactions go through the nitrophenyl group and therefore they modify the spin distribution of this part of the molecule.

The striking point on the spin density of the NO_2 group of p-NPNN is the strong positive spin population on the N2 atom. This is in direct connection with the geometrical arrangement of the molecules in this crystal structure. The distances between nitronyl groups of neighboring radicals are rather large, and direct SOMO-SOMO exchange cannot account for ferromagnetism. The interaction passes through the nitrophenyl group of another molecule, which implies much shorter distances. Type 1 contacts between the N2 site and the O1 sites of the two neighboring molecules (3.22Å) form 2D networks parallel to the (bc) plane. According to the theory of Kahn and Briat[21-22], the coupling is ferromagnetic if the interacting orbitals are orthogonal, which is the case.

In the m-NPIN molecule, the substitution of the nitro group in the meta rather than the para position inverses the signs of population of N and one of the O atoms. The magnitude of the NO_2 group distribution is of the same order in the two radicals. A bit surprising is the small negative population on O2, whereas O3 carries a relatively large positive spin density, in accordance with sign alternation picture.

The magnetic interactions pass also via the aromatic ring and modify the "natural" spin alternance observed in PNN. In p-NPNN, there is a total shift of negative spin towards the NO_2 group. Type 2 contacts link the adjacent carbon atoms C6 and C7 of the phenyl ring to the O1 site of the neighboring nitronyl nitroxide molecule (distances 3.14 Å and 3.18 Å). The density on these two adjacent carbons is negative. According to the theory, the coupling with the non orthogonal orbital of O1 is negative, but as the sign of the density is negative on the carbons, the overall intermolecular coupling is positive, connecting the 2D ferromagnetic networks into a 3D ferromagnetic network.

In m-NPIN the closest contact between adjacent molecules occurs between atom C13 of the phenyl ring and atom O1 of the imino nitroxide (3.23 Å for C13A-O1B and 3.17 Å for C13B-O1A). The expected alternation of signs on the ring is observed at the exception of carbon C13 which exhibits a positive rather than a negative spin density. The p orbitals of O1 and C13 are far from orthogonal (~ 40 and 45°). Therefore, as the

spin density is positive on both sites, the expected coupling between adjacent molecules should be antiferromagnetic, as experimentally observed.

CONCLUSION

The high quality of the polarized neutron data obtained in these experiments and the efficient data treatment techniques employed here, allowed to obtain precise quantitative results in terms of atomic spin populations. In addition, important qualitative pieces of information pertaining to the shape of the spin density distribution were obtained.

Our data provide new insight on the spin polarization phenomena and the orbital structure of the radicals Moreover, the study of the spin density transfer to the nitrophenyl group allows to give a qualitative explanation of the intermolecular magnetic interactions.

REFERENCES

1. A. Caneschi, D. Gatteschi and P. Rey , Prog. Inorg. Chem. 39, 331 (1991)
2. K. Awaga, T. Inabe, Y. Okoyama and Y. Marutama, Molec. Cryst. Liquid Cryst. 232, 79 (1991)
3. J.S. Miller and A.J. Epstein, Angew. Chem. Int. Ed. Engl. 33, 385 (1994)
4. P.M. Allemand, C. Fite, G. Srdanov, N. Keder, F. Wudl and P. Canfield, Synth. Metals 41-43, 3291 (1991)
5. P. Turek, K. Nozawa, D. Shiomi, K. Awaga, T. Inabe, Y. Maruyama and M.M. Kinoshita, Chem. Phys. Lett. 180, 327 (1991)
6. K. Awaga and Y. Maruyama, Chem. Phys. 91, 2743 (1989)
7. M.M. Kinoshita, P.Turek, M. Tamura, K. Nozawa, D. Shiomi, M. Nakazawa, M. Ishikawa, M. Takahashi, K. Awaga, T. Inabe and Y.Maruyama, Chem.Lett. 1225 (1991)
8. P. Rey and D. Luneau, to be published.
9. B. Gillon and J. Schweizer in: Molecules in Physics, Chemistry and Biology,Vol.II, edited by J. Maruani, (Kluwer, Dordrecht, 1989) p.111.
10. K. Awaga, T. Inabe, U. Nagashima and Y.Maruyama, J. Chem. Soc. Chem. Commun. 1617 (1989); see also the corrigenda in J. Chem. Soc. Chem. Commun. 520 (1990)
11. M. Wan and H. Wang, unpublished data

12. W.R. Busing, K.O. Martin and H.A. Levy, ORNL Rep. 59-4-37, Oak Ridge National Laboratory, Oak Ridge, TN (1991)
13. N.K. Hansen and P. Coppens, Acta Crystallogr. A34, 909 (1978)
14. N.J. Hehre, R.F. Stewart and J.A. Pople, J. Chem. Phys. 51, 2657 (1969)
15. R.J. Papoular and B. Gillon, Europhys. Lett. 13, 429 (1991)
16. R.J. Papoular, A. Zheludev, E. Ressouche and J. Schweizer, Acta Crystallogr. A to be published
17. A. Zheludev, V. Barone, M. Bonnet, B. Delley, A. Grand, E. Ressouche, P. Rey, R. Subra and J. Schweizer, J. Am. Chem. Soc. 116, 2019 (1994)
18. E. Ressouche, J.X. Boucherle, B. Gillon, P. Rey,J. Schweizer, J. Am. Chem. Soc. 115, 3610 (1993)
19. A. Zheludev, R.J. Papoular, E. Ressouche and J. Schweizer, Acta Crystallogr. A to be published
20. A. Zheludev, M. Bonnet, B. Delley, A. Grand, D. Luneau, L. Öhrström, E. Ressouche, P. Rey and J. Schweizer, J. Mag. Magn. Mat. to be published
21. O. Kahn and J. Briat, J. Chem. Soc. Faraday II B 72, 68 (1976)
22. O. Kahn and J. Briat, J. Chem. Soc. Faraday II B 72, 1441 (1976)